Contents lists available at ScienceDirect

Biochemistry and Biophysics Reports

The dose-effect response of combined red and infrared photobiomodulation on insulin resistance in skeletal muscle cells

Gabriela Silva [a,b], Saulo Soares da Silva [c], Dimitrius Santiago Passos Simões Fróes Guimarães [d], Marcos Vinicius da Cruz [d], Leonardo Reis Silveira [d], Etel Rocha-Vieira [a,b], Fabiano Trigueiro Amorim [e], Flavio de Castro Magalhaes [a,b,e,f,*]

[a] Multicentric Graduate Program in Physiological Sciences, Federal University of the Jequitinhonha and Mucuri Valleys – UFVJM. Rodovia MGT 367, KM 583, 5000, Alto da Jacuba, Diamantina, MG, 39100-000, Brazil
[b] Graduate Program in Health Sciences, Federal University of the Jequitinhonha and Mucuri Valleys – UFVJM. Rodovia MGT 367, KM 583, 5000, Alto da Jacuba, Diamantina, MG, 39100-000, Brazil
[c] Instituto de Ciências e Tecnologia, Federal University of the Jequitinhonha and Mucuri Valleys – UFVJM. Rodovia MGT 367, KM 583, 5000, Alto da Jacuba, Diamantina, MG, 39100-000, Brazil
[d] Centro de Pesquisa em Obesidade e Comorbidades - OCRC, Departamento de Biologia Estrutural e Funcional, Instituto de Biologia, Universidade Estadual de Campinas – UNICAMP. Rua Carl Von Linaeus, 2-238, Cidade Universitária, Campinas, SP, 13083-864, Brazil
[e] Department of Health, Exercise, and Sports Sciences, University of New Mexico – UNM. Johnson Center, B143 MSC04 2610, Albuquerque, New Mexico, 87131-0001, USA
[f] Department of Physical Education, Federal University of the Jequitinhonha and Mucuri Valleys – UFVJM. Rodovia MGT 367, KM 583, 5000, Alto da Jacuba, Diamantina, MG, 39100-000, Brazil

ARTICLE INFO

ABSTRACT

Obesity is a major public health problem and is a major contributor to the development of insulin resistance. In previous studies we observed that single-wavelength red or infrared photobiomodulation (PBM) improved insulin signaling in adipocytes and skeletal muscle of mice fed a high-fat diet, but information about the combination of different wavelengths, as well as the effect of different light doses (J/cm^2) is lacking. Therefore, the aim of this study was to investigate the effects of different doses of dual-wavelength PBM on insulin signaling in muscle cell, and explore potential mechanisms involved. Mouse myoblasts (C2C12) were differentiated into myotubes and cultured in palmitic acid, sodium oleate and L-carnitine (PAL) to induce insulin resistance high or in glucose medium (CTRL). Then, they received SHAM treatment (lights off, 0 J/cm^2) or PBM (660 + 850 nm; 2, 4 or 8 J/cm^2). PAL induced insulin resistance (assessed by Akt phosphorylation at ser473), attenuated maximal citrate synthase activity, and increased the phosphorylation of c-Jun NH(2) terminal kinase (JNK) (T183/Y185). PBM at doses of 4 or 8 J/cm^2 reversed these PAL-induced responses. Furthermore, at doses of 2, 4 or 8 J/cm^2, PBM reversed the increase in mitofusin-2 content induced by PAL. In conclusion, the combination of dual-wavelength red and infrared PBM at doses of 4 and 8 J/cm^2 improved intracellular insulin signaling in musculoskeletal cells, and this effect appears to involve the modulation of mitochondrial function and the attenuation of the activation of stress kinases.

1. Introduction

More than 2.5 billion (43 %) adults across the planet are overweight and more than 890 million (16 %) are obese [1]. It is estimated that more than 2.8 million deaths occur due to overweight or obesity each year in the world [2]. To put this number into perspective, during the ~3 years of the pandemic (from January 22, 2020, to March 10, 2023), 6,881,955 deaths were recorded associated with the SARS-CoV-2 virus

[3], which causes COVID-19. This number corresponds to an average of 2,293,985 deaths per year, less than the death rate associated with overweight and obesity yearly.

The increased availability of fatty acids, characteristic of obesity, can overload the ability cells to oxidize lipids, leading to the deposition of ectopic fat. As a consequence, there is an accumulation of lipids in the intracellular environment, which interferes with the insulin signaling process [4–8]. This interference culminates in impairments in the ability of insulin to inhibit endogenous glucose production in the liver and to stimulate glucose uptake in skeletal muscle and adipose tissues, characterizing the condition of insulin resistance [9]. Insulin resistance leads greater insulin production by pancreatic beta cells, as compensation, to maintain glycemic homeostasis. The persistence of these adaptive responses for long periods of time can lead to stress and dysfunction of beta cells, leading to their incapacity to produce enough insulin to counteract the increased insulin resistance [10], which can result in chronic hyperglycemia and overt type 2 diabetes (T2D) [11].

Although the mechanisms are not yet fully elucidated, there is evidence that mitochondrial dysfunction is associated with impairment of the intracellular insulin signaling pathway and the development of insulin resistance [12,13]. Mitochondrial dysfunction favors the intracellular accumulation of lipid intermediates, which interferes with insulin signaling, impairing glucose metabolism. Furthermore, accumulation of fatty acids interferes with intracellular insulin signaling through the activation of mitogen-activated protein kinases, also known as stress kinases. Stress kinases regulate diverse cellular functions, including proliferation, differentiation, migration and apoptosis [14]. However, they can also exert other actions, promoting changes that impair insulin signaling and, consequently, glucose metabolism [15,16].

Given the close association between mitochondrial dysfunction and insulin resistance, it is not surprising that interventions that improve mitochondrial function in skeletal muscle [17] and in adipocytes [18] have the potential to increase insulin sensitivity in these tissues and systemically. The non-pharmacological strategies traditionally used to treat insulin resistance, arguably because they improve mitochondrial function and other parameters associated with insulin resistance, are caloric restriction [19,20] and physical training [21]. However, despite good results, these interventions have low adherence among the population [22,23]. Considering the growing number of people with obesity, it is necessary to investigate other therapies for treating insulin resistance and preventing or mitigating T2D.

Photobiomodulation (PBM) is a non-invasive, non-thermal, safe, economically viable and innovative therapeutic approach [24], based on the application of low intensity light (less than or equal to 10 W/cm^2) [25]. Two important parameters that influence the photobiological effects of PBM are wavelength [26], and dose (also called energy density or fluence, and reported as joules (J)/cm^2) [27]. Red and infrared wavelengths are described as those with the greatest bioactivity [24,26, 28]. Moreover, there is evidence that the association of these wavelengths can induce better outcomes than those produced each one in isolation [29,30], as this combination might activate more or different chromophores in the irradiated tissue [31]. Thus, the use of dual-wavelength could be an interesting approach for enhancing PBM-induced beneficial effects [30]. Regarding the dose, PBM effects have been described as biphasic, as studies show null to minimal effects on low dosage, positive effects on moderate dosage, and negative effects on higher dosage [24,31].

There is *in vitro* [32] and in vivo [33]evidence that PBM improves mitochondrial function in skeletal muscle cells. The effects of PBM on mitochondrial function appear to involve the attenuation of the activation of inflammatory pathways [34,35] that contribute to the activation of stress kinases [36]. In previous work, we showed that single-wavelength red [37] or infrared [38] PBM reduced insulin resistance in adipocytes and skeletal muscle from mice fed a high fat diet (HFD). In parallel with our studies and in line with our results, Gong et al. [39,40] showed that PBM with red wavelength improved the

activation of protein kinase B (PKB/Akt) in insulin resistant 3T3-L1 adipocytes and in insulin resistant L6 myotubes, contributing to the reduction of insulin resistance in T2D models. Taken together, these findings show that PBM exerts positive effects on insulin resistance, possibly involving improvement in mitochondrial function.

Despite the promising results on insulin signaling in adipocytes and muscle cells, ideal PBM parameters need to be explored. Studies are still needed to investigate the dose-response relationship of PBM in musculoskeletal cells and the effects of PBM with the combination of dual-wavelength on the insulin signaling pathway. Furthermore, studies are needed to better elucidate the potential mechanisms involved in the insulin sensitizing effects of PBM. Thus, the aims of this study are to investigate the dose-response relationship of dual-wavelength (red and infrared) PBM on insulin resistant muscle cells. We hypothesize that dual-wavelength PBM will improve intracellular insulin signaling in insulin resistant skeletal muscle cells and there will be a biphasic dose-response relationship. Furthermore, these responses will involve improving mitochondrial function and attenuating the activation of stress kinases. To test this hypothesis, insulin resistance was induced in skeletal muscle myotubes, before they were treated with dual-wavelength PBM, at different doses (2, 4 or 8 J/cm^2).

2. Materials and methods

2.1. Experimental design

Insulin resistance was induced in myotubes for 24 h before they were exposed to dual-wavelength PBM at difference doses (0, 2, 4, or 8 J/cm^2). Fifteen minutes after PBM, cells were incubated with culture medium containing 20 mUI/mL of lispro insulin to stimulate the insulin signaling pathway or the same volume of PBS as control. Fifteen minutes later, cells were harvested for analysis. Therefore, analysis occurred 30 min after PBM [39].

2.2. Cell culture and induction of insulin resistance

For C2C12 culture, differentiation into myotubes, and the induction of insulin resistance, we followed established protocols from Yang et al. [41] and Gaster et al. [42]. C2C12 myoblasts were distributed at a density of 5 x 10^3 viable cells/cm^2 in 6 well plates. The culture medium used was DMEM - high glucose. Upon reaching high confluence, the stimulus was given for cellular differentiation of myoblasts into myotubes, using 2 % horse serum. After differentiation, the cells were incubated in culture medium containing 1 % fatty acid-free BSA, 0.5 mM palmitic acid and sodium oleate and 2 mM L-carnitine for the induction of insulin resistance. Culture medium containing 1 % BSA was used as control. Tests always took place within the same cell passages.

2.3. PBM

The PBM device used was developed in partnership with the Instituto de Ciência e Tecnologia (ICT) at Universidade Federal dos Vales do Jequitinhonha e Mucuri (UFVJM) and made with diodes arranged in clusters of 6 red LEDs (660 nm) and 6 infrared LEDs (850 nm) per well, in order to evenly illuminate all cells adhered to the bottom of the plate. In this device, the 6-well plate was positioned on top of the clustered diode arrangement, so the PBM is applied from bottom to top, and light did not have to travel through the culture medium to reach the cells (Fig. 1). In order to expose the myotubes to different doses of PBM, the exposure time was manipulated. Given the irradiance (i.e., the power density that reached the cells) was kept constant at 28.88 mW/cm^2, we exposed the cells for 69, 139, or 277 s. Because energy can be calculated from power x time (J = [mW x seconds]/1000), the fluence (energy density or dose, in J/cm^2) was 2, 4, and 8 J/cm^2 for the exposure of 69, 139, and 277 s, respectively. The parameters used are described in Table 1. For the present study, diodes from both wavelengths were
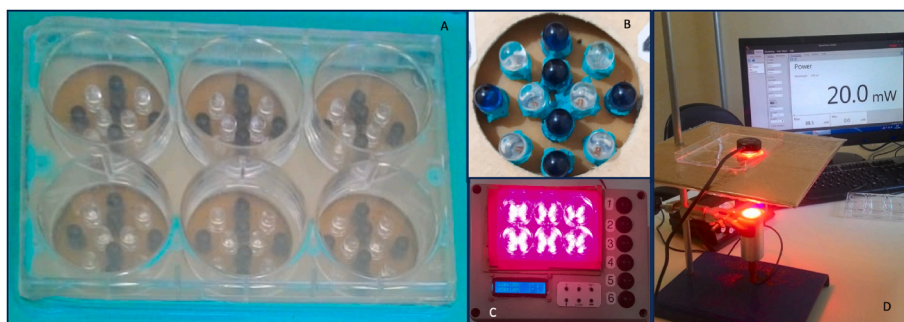
Fig. 1. PBM device in C2C12 myotubes. A: Each individual well was illuminated by a cluster of 12 LED diodes (6 red – 660 nm, and 6 infrared – 850 nm). B: Detailed arrangement of the diodes. C: Device in operation. D: example of optical power being assessed. (For interpretation of the references to colour in this figure legend, the reader is referred to the Web version of this article.)

Table 1
PBM parameters in C2C12 myotubes.

Wavelengths	660 nm (red)			850 nm (infrared)			Combined		
Number of diodes per well	6			6			12		
Pulse frequency	continuous								
Application mode	2.6 cm away from the plate								
Sensor area (cm^2)	0.71								
Radiant flux at the sensor (mW)	6.5			14			19.5		
Irradiance at the sensor (mW/cm^2)	9.16			19.72			28.88		
Exposure time (seg)	69	139	277	69	139	277	69	139	277
Fluence (J/cm^2)	0.63	1.27	2.54	1.36	2.74	5.46	2	4	8
Well area (cm^2)	9.6								
Radiant energy (J) per well	6.1	12.2	24.4	13.1	26.3	52.4	19.2	38.5	76.8

Nm – nanometer; cm – centimeter; mW – miliwatt; seg – second; J – joule. For the present study diodes from both wavelengths were turned on, so the combined column represents.

turned on, as we aimed to assess the effects of the combined red and infrared PBM on insulin signaling, as this dual-wavelength approach can induce better responses than either wavelength in isolation [30]. Thus, the combined (third) column in Table 1 represents the parameters used.

The optical power was measured with the aid of power meter (PM100USB, Thorlabs®) attached to a sensor S121C (Thorlabs®). The sensor was positioned inside each individual well (Fig. 1D) and the well was illuminated from underneath, to take into account the potential interference of the acrylic material of the well, mimicking the light that would actually reach the cell adhered to the bottom of the well. The values shown in Table 1 represent the results for the optical power assessments. Furthermore, the diodes were tested for peak wavelength and spectral band size. The 660 nm diode had a peak emission at 665.25 nm, with a spectral band size (±50 % of the peak) of 23.5 nm. The 850 nm diode 850 had a peak emission at 850.3 nm, and a spectral band size of 45.68 nm. From these data it is possible to state that the light emission was within the expected ranges for the diodes used.

2.4. Temperature during PBM application

The plate containing myotubes and culture medium was exposed to PBM using exactly the same parameters defined for the cell experiments, and a digital multimeter sensor (Pol-41, Politerm) was inserted into the well, in direct contact with the cells and the culture medium. This process was carried out in three different wells. In the first, the sensor was kept against the side acrylic of the inner part of the well and the application time was 69 s, in the second, it was placed in the central region and the application time was 139 s, and in the third, it was positioned intermediately between these two portions and the application time was 277 s. The temperature (°C), displayed on the device monitor, was recorded.

2.5. Cell viability

The tests took place 30 min after the PBM. Trypan blue solution (0.4 %) was diluted in a 1:1 ratio with each sample. Then, 10 μL of this final solution was added to the Neubauer chamber to count viable (unstained) and non-viable (stained) cells under an inverted microscope. To calculate the percentage of viable cells, the number of viable cells was divided by the total number of cells and the result of this division was multiplied by 100.

2.6. Protein content and phosphorylation

The culture medium was removed and extraction buffer was added to each well. The cells were removed using a cell scraper and the entire volume was collected in identified tubes. The tubes were placed on ice and each sample was homogenized with a pipette in 6 cycles of 20 up-down. The lysates were centrifuged at 12000 g for 5 min at 4 °C and the supernatant was collected.

Protein content and phosphorylation were analyzed using the Western ImmunoBlotting technique. For a detailed description see Silva et al. [37,38]. Briefly, samples were run in SDS-PAGE and transferred to PVDF membranes. The following primary antibodies were used (1:1000): phospho-Akt (Ser473), total Akt, Mitofusin-2, GAPDH, phospho-SAPK/JNK (Thr183/Tyr185), total SAPK/JNK (all from Cell Signaling). The membranes were then incubated with anti-rabbit IgG secondary antibody (1:5000; Cell Signaling). Band density was quantified using ImageJ software. The relative content values generated are presented as arbitrary units.

2.7. Citrate synthase activity

To analyze the maximum activity of citrate synthase in C2C12 myotubes, 100 μL of extraction buffer were added to tubes containing

10^6 cells. The tubes were placed on ice and each sample was homogenized, with a P200 pipette, in 6 cycles of 20 up-down. The lysates were centrifuged at 10000 g for 20 min at 4 °C to separate cellular debris. Aliquots of supernatant were separated for measurement of total proteins and for the enzymatic assay. The concentration of total proteins in the extracts was determined using the Bradford technique [43]. The reading was carried out in a microplate reader at a wavelength of 595 nm. Protein values were determined using the Softmaxpro® software, in mg/mL. The maximum activity of the enzyme was determined according to a modified protocol [44–46], from the quantification of the yellow complex formed between the CoA released in the reaction with 5, 5-dithiobis(2-nitrobenzoic acid) (DTNB) (Ellman reagent) present in the assay buffer. To visualize the enzymatic activity curve up to the maximum point of the reaction, 48 readings were taken with 5 s intervals between them, at 25 °C. The assay was carried out in triplicate of each sample and the average of the 3 values obtained per sample was used for the calculation. The values were multiplied by one thousand (1000) and the results were expressed in nmol/min/mg of protein.

2.8. Statistical analysis

For statistical analysis, the Statistica software was used. The Shapiro-Wilk test was performed to assess data normality. A 3-way analysis of variance (ANOVA) was used. When significant differences were detected, the tests were followed by Fisher LSD post-hoc for specific detection of differences. The significance level adopted was $p < 0.05$. The results are presented as mean ± standard error.

3. Results and discussion

3.1. Temperature during PBM application

Tissues heating is associated with improvement in glucose metabolism. For instance, exposure to heat increased mitochondrial biogenesis in C2C12 myotubes [47], and mitochondrial biogenesis and function in human skeletal muscle tissue [48], activated mitochondrial enzymes in rat skeletal muscle tissue [49], improved insulin sensitivity in skeletal muscle tissue of HFD-fed rats [50], protected against HDF-induced insulin resistance in skeletal muscle of mice [51] and improved insulin sensitivity in adipose tissue of women with polycystic ovary syndrome [52]. No change was observed in the temperature measured in wells containing culture media and cells, as shown in Table 2, which suggests that temperature did not affect the present results.

3.2. Cell viability

The percentage of viable cells was greater than 90 % in all groups (Fig. 2), and no difference was observed among groups. Therefore, the induction of insulin resistance with palmitate, sodium oleate and L-carnitine, treatment with PBM, and incubation with insulin did not alter the viability of C2C12 myotubes.

3.3. Protein content and phosphorylation

Akt is a key enzyme in insulin signaling and impairment in its activity is associated with a reduction in glucose uptake, characterizing the condition of insulin resistance [16]. In fact, humans with insulin
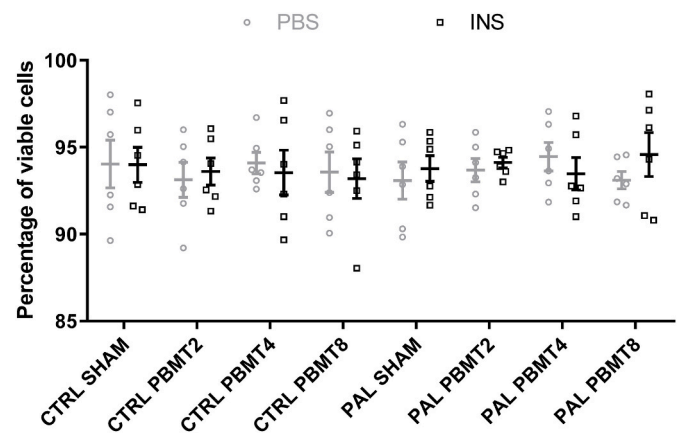

Fig. 2. Cellular viability of C2C12 myotubes. Effect of CTRL or PAL media and SHAM or PBM2 or PBM4 or PBM8 treatment and PBS or INS stimulation on cell viability. Groups: CTRL-SHAM-PBS (n = 6); CTRL-SHAM-INS (n = 6); CTRL-PBM2-PBS (n = 6); CTRL-PBM2-INS (n = 6); CTRL-PBM4-PBS (n = 6); CTRL-PBM4-INS (n = 6); CTRL-PBM8-PBS (n = 6); CTRL-PBM8-INS (n = 6); PAL-SHAM-PBS (n = 6); PAL-SHAM-INS (n = 6); PAL-PBM2-PBS (n = 6); PAL-PBM2-INS (n = 6); PAL-PBM4-PBS (n = 6); PAL-PBM4-INS (n = 6); PAL-PBM8-PBS (n = 6); PAL-PBM8-INS (n = 6).

resistance and T2D have a deficiency in Akt activation, associated with a reduction in glucose uptake [53–59]. Impairment in Akt activity has already been demonstrated in the skeletal muscle of rodents fed with HFD [60–62] and in C2C12 cells treated with palmitate [4,63]. Furthermore, Akt phosphorylation at ser473 is dramatically and negatively affected in insulin resistant states [4,39–41,64,65].

In the present study, we evaluated the phosphorylation of Akt (ser 473) in C2C12 myotubes (Fig. 3) and, corroborating the aforementioned studies, we also observed a reduction in the activation of this protein in response to PAL, which characterizes the induction of insulin resistance. PBM, at doses of 4 or 8 J/cm², completely reversed this reduction, suggesting that insulin sensitivity was reestablished. Therefore, the present study shows, for the first time, the effects of PBM, with the combination of red and infrared wavelengths, in different doses, on the insulin signaling pathway. This result expands our previous study [38] and shows that PBM reverses insulin resistance not only in adipocytes, but also in myotubes. These data are in line with the findings of Gong et al. [40], who also observed increased activation of the insulin pathway in skeletal muscle, with consequent improvement in glucose metabolism after red PBM in a mouse model with T2D and in insulin resistance L6 myotubes. Although it is not completely understood the mechanism by which PBM stimulates Akt phosphorylation, there is evidence that in insulin resistant skeletal muscles, PBM accelerates cytochrome c oxidase activity, and stimulates the production of reactive oxygen species, which activates the phosphatase and tensin homolog/Akt pathway [40].

One of the factors that can interfere with insulin signaling, as a result of lipid overload, is the activation of stress kinases, such as JNK, which promotes the phosphorylation of serine and threonine residues of IRS1, inhibiting the pathway [15]. In cultured myocytes, it has been demonstrated that palmitate-induced insulin resistance is accompanied by an increase in JNK activation [66], while JNK knockdown attenuates palmitate-induced insulin resistance [67]. In mice and humans with

Table 2
Temperature during PBM application.

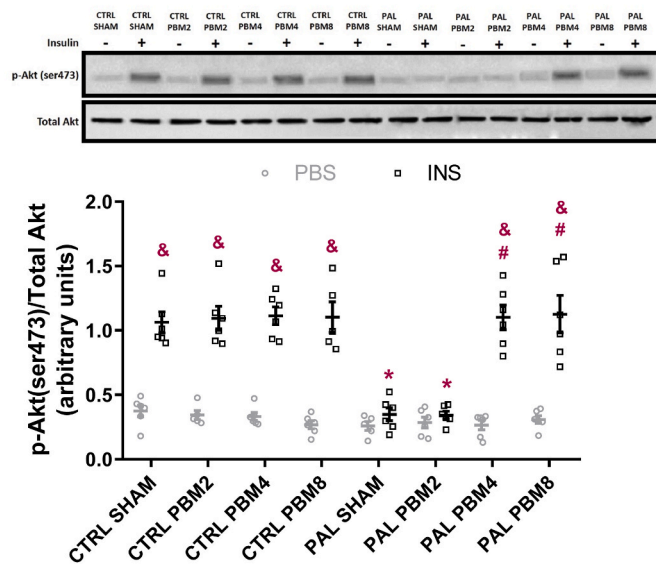| Well region	Time (s)	Initial temperature (°C)	Final temperature (°C)	Delta (°C)
1 - side	69	24	24	0
2 - center	139	24	24	0
3 - intermediate	277	24	24	0

Fig. 3. Phosphorylation of Akt (ser473) in C2C12 myotubes. Effect of CTRL or PAL media and SHAM or PBM2 or PBM4 or PBM8 treatment and PBS (−) or INS (+) stimulation on Akt (ser473) phosphorylation. *p < 0.05 vs CTRL; #p < 0.05 vs PAL-SHAM e PAL-PBM2; & p < 0.05 vs PBS. Groups: CTRL-SHAM-PBS (n = 6); CTRL-SHAM-INS (n = 6); CTRL-PBM2-PBS (n = 5); CTRL-PBM2-INS (n = 6); CTRL-PBM4-PBS (n = 6); CTRL-PBM4-INS (n = 6); CTRL-PBM8-PBS (n = 6); CTRL-PBM8-INS (n = 5); PAL-SHAM-PBS (n = 5); PAL-SHAM-INS (n = 6); PAL-PBM2-PBS (n = 6); PAL-PBM2-INS (n = 6); PAL-PBM4-PBS (n = 6); PAL-PBM4-INS (n = 6); PAL-PBM8-PBS (n = 6); PAL-PBM8-INS (n = 6).

Fig. 4. Phosphorylation of JNK (thr183/tyr185) in C2C12 myotubes. Effect of CTRL or PAL media and SHAM or PBM2 or PBM4 or PBM8 treatment and PBS (−) or INS (+) stimulation on JNK (thr183/tyr185) phosphorylation. *p < 0.05 vs CTRL; #p < 0.05 vs PAL-SHAM e PAL-PBM2. Grupos: CTRL-SHAM-PBS (n = 6); CTRL-SHAM-INS (n = 6); CTRL-PBM2-PBS (n = 6); CTRL-PBM2-INS (n = 5); CTRL-PBM4-PBS (n = 6); CTRL-PBM4-INS (n = 6); CTRL-PBM8-PBS (n = 6); CTRL-PBM8-INS (n = 6); PAL-SHAM-PBS (n = 6); PAL-SHAM-INS (n = 6); PAL-PBM2-PBS (n = 6); PAL-PBM2-INS (n = 6); PAL-PBM4-PBS (n = 5); PAL-PBM4-INS (n = 6); PAL-PBM8-PBS (n = 6); PAL-PBM8-INS (n = 6).

obesity, JNK activity is also increased in skeletal muscle [15,68,69]. Three different genes encode for 3 different JNK isoforms: JNK 1, 2 and 3 [70], and studies point to JNK 1 as the isoform that most contributes to the development of insulin resistance associated with obesity, since knockdown mice for JNK 1, but not for JNK 2, are considerably protected from obesity and insulin resistance, in models of diet- and genetically-induced obesity [15,36].

In this research, we evaluated the activation of JNK (1/2) in C2C12 myotubes (Fig. 4) and, in line with the aforementioned studies, we observed increased activation in response to PAL. This increase was completely reversed by PBM at doses of 4 or 8 J/cm^2. Previously, we demonstrated that infrared PBM partially inhibited JNK activation in adipose tissue in mice fed a HFD [38]. In another study, we also showed that red PBM completely reversed the increase in JNK activation induced by HFD in the adipose tissue of mice [37]. Along the same line, it has been demonstrated that infrared PBM reduced the increased JNK activation in response to restraint stress in the prefrontal cortex of mice [71]. Thus, PBM reduces JNK activation, and this reduction might be at least one of the mechanisms the PBM can improve glucose metabolism.

Another factor closely associated with insulin resistance is the reduction of mitochondrial biogenesis and function [12] that can be improved by PBM [29,33,72,73]. Therefore, we investigated the content of a mitochondrial protein, mitofusin-2. The morphology of mitochondria is constantly changing through the processes of fusion and fission [74] and Littlejohns et al. [75] suggested that these processes are important for the regulation of insulin resistance. In the present study, we observed that myotubes maintained in PAL showed an increase in mitofusin-2 content and that PBM, at doses of 2, 4 or 8 J/cm^2, completely inhibited the increase in mitofusin-2 (Fig. 5).

Our results contrast with those of some studies that show a reduction in the content of the mitofusin-2 protein in skeletal muscle in obese Zucker rats [76], individuals with obesity and patients with T2D [77] and HFD-fed rats [78]. On the other hand, and consistent with our findings, Littlejohns et al. [75] observed an increase in mitofusin-2 content in cardiac tissue from HFD-fed mice, in parallel with a
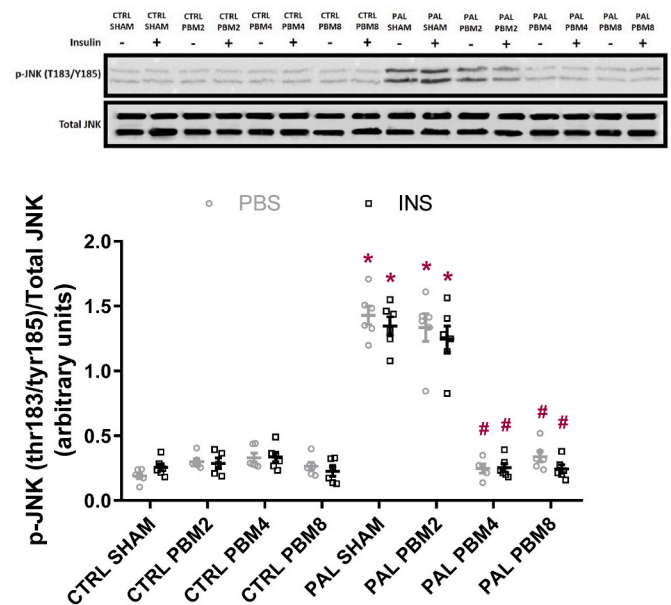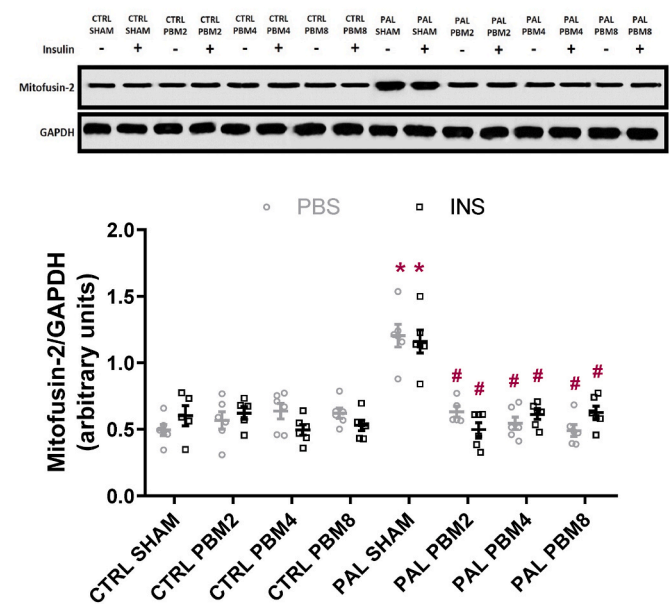

Fig. 5. Mitofusin-2 content in C2C12 myotubes. Effect of CTRL or PAL medium and SHAM or PBM2 or PBM4 or PBM8 treatment and PBS (−) or INS (+) stimulation on mitofusin-2 content. *p < 0.05 vs CTRL; #p < 0.05 vs PAL-SHAM. Groups: CTRL-SHAM-PBS (n = 6); CTRL-SHAM-INS (n = 5); CTRL-PBM2-PBS (n = 6); CTRL-PBM2-INS (n = 5); CTRL-PBM4-PBS (n = 6); CTRL-PBM4-INS (n = 6); CTRL-PBM8-PBS (n = 6); CTRL-PBM8-INS (n = 6); PAL-SHAM-PBS (n = 6); PAL-SHAM-INS (n = 6); PAL-PBM2-PBS (n = 5); PAL-PBM2-INS (n = 6); PAL-PBM4-PBS (n = 6); PAL-PBM4-INS (n = 6); PAL-PBM8-PBS (n = 6); PAL-PBM8-INS (n = 6).

reduction in the area, length and density of cardiac mitochondria. Furthermore, mitofusin-2 protein content in the skeletal muscle was increased in older compared to younger individuals [78], despite the fact that mitochondrial dysfunction is associated with aging [79–81]. Also, when subjected to chronic high-intensity aerobic training, these older individuals had reduced mitofusin-2, but increased mitochondrial content. Thus, it would be reasonable to speculate that as the subjects aged, there was an increase in mitofusin-2 to counteract mitochondrial dysfunction. Conversely, as they became physically trained, and mitochondrial function improved, mitofusin-2 decreased. Similarly, in the present study, mitofusin-2 might have been increased by PAL to compensate for the worsening of mitochondrial function, while PBM caused both an improvement in mitochondrial function, along with a reduction in mitofusin-2.

3.4. Citrate synthase activity

Citrate synthase is an enzyme that participates in oxidative metabolism and has been used as a biomarker of mitochondrial content and function [82,83]. In this study, we observed that PBM, at doses of 4 or 8 J/cm^2, completely reversed the reduction in the maximum activity of citrate synthase in response to insulin, caused by PAL, reestablishing the response of this enzyme to insulin (Fig. 6).

The study by Ørtenblad et al. [84] also showed that citrate synthase activity from myotubes established from individuals with T2D were insensitive to insulin stimulation. Conversely, insulin stimulated citrate synthase activity by 26–33 % in myotubes established from lean control and obese individuals, and this stimulatory effect of insulin was abolished by high concentrations of palmitate. According to them, a likely mechanism for the change in citrate synthase activity in response to insulin is the phosphorylation/dephosphorylation of this protein.

Regarding the effects of PBM on citrate synthase, our results corroborate those of Aquino et al. [85] who observed an increase in citrate synthase activity induced by infrared PBM in the skeletal muscle of rats. In line with these findings, the study by Vieira et al. [86] also showed an increase in mitochondrial citrate synthase activity induced by infrared PBM in the skeletal muscle of rats subjected to aerobic
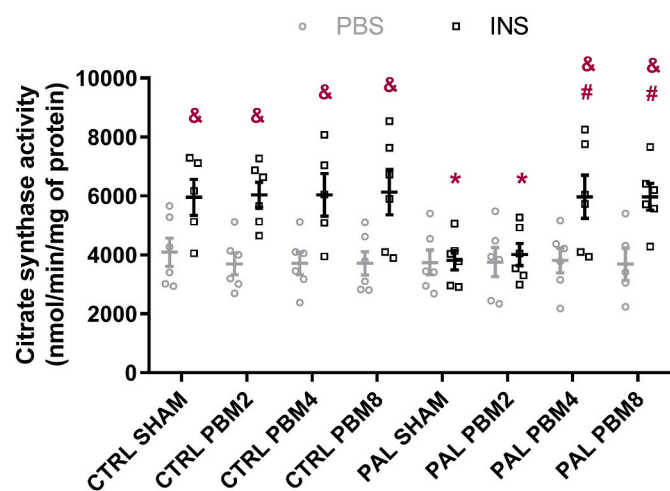
training. Taken together, these data show that PBM increases citrate synthase activity in mouse and rat musculoskeletal cells.

Together, the results of mitofusin-2 and citrate synthase suggest that the excessive supply of lipids in PAL impaired mitochondrial oxidative capacity. In response, mitochondrial dynamics increased (i.e., mitofusin-2 content increased). However, this adaptive response insufficiently compensated for the increase in lipid availability, leading to insulin resistance, including at the level of citrate synthase. In this context, the Krebs cycle appears to have been a limiting point for this compensatory response. In contrast, PBM reduced insulin resistance, probably reducing lipotoxicity and improving mitochondrial function. This reestablished the activation of citrate synthase by insulin and attenuated the stimulus for mitofusin-2. Further studies are needed to confirm whether the changes observed in citrate synthase and mitofusin-2 translate into changes in mitochondrial function and morphology, respectively.

The main finding of this study is that the effects of dual-wavelength PBM on musculoskeletal cells were dependent on the dose, similar to what was observed by Gong et al. [39], who used red PBM in fat cells. The effect on Akt activation was only observed with doses of 4 or 8 J/cm^2, similar to the study mentioned, as well as for the effects on the maximum activity of citrate synthase and activation of JNK. However, the effects on mitofusin-2 content were observed both with doses of 2, 4 or 8 J/cm^2. According to the Arndt-Schultz law, small doses are not sufficient to generate relevant biological effects [24,31]. Our data aligns with the Arndt-Schultz law as the dose of 2 J/cm^2 was not sufficient to we cause alterations in most parameters assessed, while 4 and 8 were.

In conclusion, confirming our hypothesis, PBM improved intracellular insulin signaling in musculoskeletal cells in an *in vitro* experimental model of lipid overload with the combination of red and infrared wavelengths. This effect appears to depend on the dose and to be related to other changes promoted by PBM, such as the modulation of mitochondrial function and the attenuation of the activation of stress kinases. These results add to studies in rodent models [34,37–40,87,88] and in humans [89–91] showing improvements in glucose metabolism following PBM treatment, and suggest that dual-wavelength PBM might be a suitable treatment option for individuals living with insulin resistance.

Fig. 6. Maximum citrate synthase activity in C2C12 myotubes. Effect of CTRL or PAL medium and SHAM or PBM2 or PBM4 or PBM8 treatment and PBS (−) or INS (+) stimulation on maximal citrate synthase activity. *p < 0.05 vs CTRL; #p < 0.05 vs PAL-SHAM e PAL-PBM2; & p < 0.05 vs PBS. Groups: CTRL-SHAM-PBS (n = 6); CTRL-SHAM-INS (n = 5); CTRL-PBM2-PBS (n = 6); CTRL-PBM2-INS (n = 6); CTRL-PBM4-PBS (n = 6); CTRL-PBM4-INS (n = 5); CTRL-PBM8-PBS (n = 6); CTRL-PBM8-INS (n = 6); PAL-SHAM-PBS (n = 6); PAL-SHAM-INS (n = 6); PAL-PBM2-PBS (n = 6); PAL-PBM2-INS (n = 6); PAL-PBM4-PBS (n = 6); PAL-PBM4-INS (n = 6); PAL-PBM8-PBS (n = 5); PAL-PBM8-INS (n = 6).

CRediT authorship contribution statement

Gabriela Silva: Writing – original draft, Methodology, Formal analysis, Conceptualization. **Saulo Soares da Silva:** Methodology. **Dimitrius Santiago Passos Simões Fróes Guimarães:** Methodology. **Marcos Vinicius da Cruz:** Methodology. **Leonardo Reis Silveira:** Writing – review & editing, Methodology. **Etel Rocha-Vieira:** Methodology. **Fabiano Trigueiro Amorim:** Methodology. **Flavio de Castro Magalhães:** Writing – review & editing, Supervision, Project administration, Methodology, Funding acquisition, Formal analysis, Conceptualization.

Declaration of competing interest

The authors declare that they have no known competing financial interests or personal relationships that could have appeared to influence the work reported in this paper.

Data availability

Data will be made available on request.

Appendix A. Supplementary data

Supplementary data to this article can be found online at https://doi.org/10.1016/j.bbrep.2024.101831.

References

[1] World Health Organization (WHO), Obesity and overweight. https://www.Who.Int/News-Room/Fact-Sheets/Detail/Obesity-and-Overweight, 2024.

[2] WHO - WORLD HEALTH ORGANIZATION, Obesity (2021). https://www.Who.Int/News-Room/Facts-in-Pictures/Detail/6-Facts-on-Obesity#:~:Text=In%202016%2C%20more%20than%201.9,Of%20being%20overweight%20or%20obese.

[3] J.H.U.& M. (JHU) JHU, COVID-19 dashboard by the center for systems science and engineering (CSSE) at johns hopkins university (JHU). https://Coronavirus.Jhu.Edu/Map.Html, 2023.

[4] J.A. Chavez, S.A. Summers, Characterizing the effects of saturated fatty acids on insulin signaling and ceramide and diacylglycerol accumulation in 3T3-L1 adipocytes and C2C12 myotubes, Arch. Biochem. Biophys. 419 (2003) 101–109, https://doi.org/10.1016/j.abb.2003.08.020.

[5] J. Davis, N. Gabler, J. Walker-Daniels, M. Spurlock, The c-jun N-terminal kinase mediates the induction of oxidative stress and insulin resistance by palmitate and toll-like receptor 2 and 4 ligands in 3T3-L1 adipocytes, Horm. Metab. Res. 41 (2009) 523–530, https://doi.org/10.1055/s-0029-1202852.

[6] W.L. Holland, B.T. Bikman, L.-P. Wang, G. Yuguang, K.M. Sargent, S. Bulchand, T. A. Knotts, G. Shui, D.J. Clegg, M.R. Wenk, M.J. Pagliassotti, P.E. Scherer, S. A. Summers, Lipid-induced insulin resistance mediated by the proinflammatory receptor TLR4 requires saturated fatty acid–induced ceramide biosynthesis in mice, J. Clin. Invest. 121 (2011) 1858–1870, https://doi.org/10.1172/JCI43378.

[7] R. Hage Hassan, A.C. Pacheco de Sousa, R. Mahfouz, I. Hainault, A. Blachnio-Zabielska, O. Bourron, J. Górski, P. Ferré, F. Foufelle, E. Hajduch, Sustained action of ceramide on the insulin signaling pathway in muscle cells: implication of the double-stranded rna-activated protein kinase, J. Biol. Chem. 291 (2016) 3019–3029, https://doi.org/10.1074/jbc.M115.686949.

[8] H. Shi, M.V. Kokoeva, K. Inouye, I. Tzameli, H. Yin, J.S. Flier, TLR4 links innate immunity and fatty acid–induced insulin resistance, J. Clin. Invest. 116 (2006) 3015–3025, https://doi.org/10.1172/JCI28898.

[9] V.T. Samuel, G.I. Shulman, The pathogenesis of insulin resistance: integrating signaling pathways and substrate flux, J. Clin. Invest. 126 (2016) 12–22, https://doi.org/10.1172/JCI77812.

[10] A. Clark, L.C. Jones, E. de Koning, B.C. Hansen, D.R. Matthews, Decreased insulin secretion in type 2 diabetes: a problem of cellular mass or function? Diabetes 50 (2001) S169, https://doi.org/10.2337/diabetes.50.2007.S169.

[11] K. Shim, R. Begum, C. Yang, H. Wang, Complement activation in obesity, insulin resistance, and type 2 diabetes mellitus, World J. Diabetes (2020), https://doi.org/10.4239/wjd.v11.i1.1.

[12] M.K. Montgomery, N. Turner, Mitochondrial dysfunction and insulin resistance: an update, Endocr Connect 4 (2015), https://doi.org/10.1530/EC-14-0092.

[13] D. Sergi, N. Naumovski, L.K. Heilbronn, M. Abeywardena, N. O'Callaghan, L. Lionetti, N. Luscombe-Marsh, Mitochondrial (Dys)function and insulin resistance: from pathophysiological molecular mechanisms to the impact of diet, Front. Physiol. 10 (2019), https://doi.org/10.3389/fphys.2019.00532.

[14] P.W. Vesely, P.B. Staber, G. Hoefler, L. Kenner, Translational regulation mechanisms of AP-1 proteins, Mutation Research/Reviews in Mutation Research 682 (2009) 7–12, https://doi.org/10.1016/j.mrrev.2009.01.001.

[15] J. Hirosumi, G. Tuncman, L. Chang, C.Z. Görgün, K.T. Uysal, K. Maeda, M. Karin, G.S. Hotamisligil, A central, role for JNK in obesity and insulin resistance, Nature 420 (2002) 333–336, https://doi.org/10.1038/nature01137.

[16] P. Dandona, Inflammation: the link between insulin resistance, obesity and diabetes, Trends Immunol. 25 (2004) 4–7, https://doi.org/10.1016/j.it.2003.10.013.

[17] A.R. Martins, R.T. Nachbar, R. Gorjao, M.A. Vinolo, W.T. Festuccia, R. H. Lambertucci, M.F. Cury-boaventura, L.R. Silveira, R. Curi, S.M. Hirabara, Mechanisms underlying skeletal muscle insulin resistance induced by fatty acids : importance of the mitochondrial function, Lipids Health Dis. 11 (2012) 30, https://doi.org/10.1186/1476-511X-11-30.

[18] C.M. Kusminski, P.E. Scherer, Mitochondrial dysfunction in white adipose tissue, Trends in Endocrinology & Metabolism 23 (2012) 435–443, https://doi.org/10.1016/j.tem.2012.06.004.

[19] A.E. Civitarese, S. Carling, L.K. Heilbronn, M.H. Hulver, B. Ukropcova, W. A. Deutsch, S.R. Smith, E. Ravussin, C. Pennington, Calorie restriction increases muscle mitochondrial biogenesis in healthy humans, 4, https://doi.org/10.1371/journal.pmed.0040076, 2007.

[20] E. Nisoli, C. Tonello, A. Cardile, V. Cozzi, R. Bracale, L. Tedesco, S. Falcone, A. Valerio, O. Cantoni, E. Clementi, S. Moncada, M.O. Carruba, Cell biology: calorie restriction promotes mitochondrial biogenesis by inducing the expression of eNOS, Science (1979), https://doi.org/10.1126/science.1117728, 2005.

[21] F.G.S. Toledo, E.V. Menshikova, V.B. Ritov, K. Azuma, Z. Radikova, J. DeLany, D. E. Kelley, Effects of physical activity and weight loss on skeletal muscle mitochondria and relationship with glucose control in type 2 diabetes, Diabetes 56 (2007) 2142–2147, https://doi.org/10.2337/db07-0141.

[22] V.A. Catenacci, H.R. Wyatt, The role of physical activity in producing and maintaining weight loss, Nat Clin Pract Endocrinol Metab 3 (2007) 518–529, https://doi.org/10.1038/ncpendmet0554.

[23] M. Blüher, Obesity: global epidemiology and pathogenesis, Nat. Rev. Endocrinol. (2019), https://doi.org/10.1038/s41574-019-0176-8.

[24] M.R. Hamblin, Mechanisms and applications of the anti-inflammatory effects of photobiomodulation, AIMS Biophys 4 (2017) 337–361, https://doi.org/10.3934/biophy.2017.3.337.

[25] W. Posten, D.A. Wrone, J.S. Dover, K.A. Arndt, S. Silapunt, M. Alam, Low-level laser therapy for wound healing: mechanism and efficacy, Dermatol. Surg. (2005), https://doi.org/10.1097/00042728-200503000-00016.

[26] M.R. Hamblin, T.N. Demidova, Mechanisms of low level light therapy, in: M. R. Hamblin, R.W. Waynant, J. Anders (Eds.), Mechanisms for Low-Light Therapy, 2006 614001, https://doi.org/10.1117/12.646294.

[27] R. Zein, W. Selting, M.R. Hamblin, Review of light parameters and photobiomodulation efficacy: dive into complexity, J. Biomed. Opt. 23 (2018) 1, https://doi.org/10.1117/1.jbo.23.12.120901.

[28] T.I. Karu, Multiple roles of cytochrome c oxidase in mammalian cells under action of red and IR-A radiation, IUBMB Life 62 (2010) 607–610, https://doi.org/10.1002/iub.359.

[29] F. de C. Magalhães, C. Ferraresi, Photobiomodulation therapy on the treatment of insulin resistance: a narrative review, Photobiomodul Photomed Laser Surg (2022), https://doi.org/10.1089/photob.2022.0031.

[30] A.M.C.T. Lima, L.P. da Silva Sergio, A. de Souza da Fonseca, Photobiomodulation via multiple-wavelength radiations, Lasers Med Sci 35 (2020) 307–316, https://doi.org/10.1007/s10103-019-02879-1.

[31] H. Chung, T. Dai, S.K. Sharma, Y.Y. Huang, J.D. Carroll, M.R. Hamblin, The nuts and bolts of low-level laser (Light) therapy, Ann. Biomed. Eng. 40 (2012) 516–533, https://doi.org/10.1007/s10439-011-0454-7.

[32] C. Ferraresi, B. Kaippert, P. Avci, Y.Y. Huang, M.V.P. De Sousa, V.S. Bagnato, N. A. Parizotto, M.R. Hamblin, Low-level laser (light) therapy increases mitochondrial membrane potential and ATP synthesis in C2C12 myotubes with a peak response at 3-6 h, Photochem. Photobiol. 91 (2015) 411–416, https://doi.org/10.1111/php.12397.

[33] P.C.L. Silveira, G.K. Ferreira, R.P. Zaccaron, V. Glaser, A.P. Remor, C. Mendes, R. A. Pinho, A. Latini, Effects of photobiomodulation on mitochondria of brain, muscle, and C6 astroglioma cells, Med. Eng. Phys. 71 (2019) 108–113, https://doi.org/10.1016/j.medengphy.2019.05.008.

[34] T.M. Yoshimura, C.P. Sabino, M.S. Ribeiro, Photobiomodulation reduces abdominal adipose tissue inflammatory infiltrate of diet-induced obese and hyperglycemic mice, J Biophotonics 9 (2016) 1255–1262, https://doi.org/10.1002/jbio.201600088.

[35] T.C. dos Santos, K. de Brito Sousa, L. Andreo, A. Martinelli, M.F.S.D. Rodrigues, S. K. Bussadori, K.P.S. Fernandes, R.A. Mesquita-Ferrari, Effect of photobiomodulation on C2C12 myoblasts cultivated in M1 macrophage-conditioned media. https://doi.org/10.1111/php.13215, 2020.

[36] G. Tuncman, J. Hirosumi, G. Solinas, L. Chang, M. Karin, G.S. Hotamisligil, Functional in vivo interactions between JNK1 and JNK2 isoforms in obesity and insulin resistance, Proc. Natl. Acad. Sci. USA 103 (2006) 10741–10746, https://doi.org/10.1073/pnas.0603509103.

[37] G. Silva, C. Ferraresi, R.T. Almeida, M.L. Motta, T. Paixão, V.O. Ottone, I. A. Fonseca, M.X. Oliveira, E. Rocha-Vieira, M.F. Dias-Peixoto, E.A. Esteves, C. C. Coimbra, F.T. Amorim, F. de C. Magalhães, Insulin resistance is improved in high-fat fed mice by photobiomodulation therapy at 630 nm, J. Biophot. 13 (2020) 1–16, https://doi.org/10.1002/jbio.201960140.

[38] G. Silva, C. Ferraresi, R.T. de Almeida, M.L. Motta, T. Paixão, V.O. Ottone, I. A. Fonseca, M.X. Oliveira, E. Rocha-Vieira, M.F. Dias-Peixoto, E.A. Esteves, C. C. Coimbra, F.T. Amorim, F. de Castro Magalhães, Infrared photobiomodulation (PBM) therapy improves glucose metabolism and intracellular insulin pathway in adipose tissue of high-fat fed mice, Lasers Med Sci 33 (2018) 559–571, https://doi.org/10.1007/s10103-017-2408-2.

[39] L. Gong, Z. Zou, L. Huang, S. Guo, D. Xing, Photobiomodulation therapy decreases free fatty acid generation and release in adipocytes to ameliorate insulin resistance

in type 2 diabetes, Cell. Signal. 67 (2020) 109491, https://doi.org/10.1016/j.cellsig.2019.109491.

[40] L. Gong, Z. Zou, L. Liu, S. Guo, D. Xing, Photobiomodulation therapy ameliorates hyperglycemia and insulin resistance by activating cytochrome c oxidase-mediated protein kinase B in muscle, Aging 13 (2021) 10015–10033, https://doi.org/10.18632/aging.202760.

[41] M. Yang, D. Wei, C. Mo, J. Zhang, X. Wang, X. Han, Z. Wang, H. Xiao, Saturated fatty acid palmitate-induced insulin resistance is accompanied with myotube loss and the impaired expression of health benefit myokine genes in C2C12 myotubes, Lipids Health Dis. 12 (2013) 104, https://doi.org/10.1186/1476-511X-12-104.

[42] M. Gaster, A.C. Rustan, V. Aas, H. Beck-Nielsen, Reduced lipid oxidation in skeletal muscle from type 2 diabetic subjects may Be of genetic origin, Diabetes 53 (2004) 542–548, https://doi.org/10.2337/diabetes.53.3.542.

[43] M. Bradford, A rapid and sensitive method for the quantitation of microgram quantities of protein utilizing the principle of protein-dye binding, Anal. Biochem. 72 (1976) 248–254, https://doi.org/10.1006/abio.1976.9999.

[44] P.R. Alp, E.A. Newsholme, V.A. Zammit, Activities of citrate synthase and NAD+ linked and NADP+ linked isocitrate dehydrogenase in muscle from vertebrates and invertebrates, Biochem. J. 154 (1976) 689–700, https://doi.org/10.1042/bj1540689.

[45] F. de Castro Magalhães, T. Fernandes, V. Bassaneze, K.C. Mattos, I. Schettert, F.L. N. Marques, J.E. Krieger, R. Nava, V.G. Barauna, E.M. de Oliveira, High-volume endurance exercise training stimulates hematopoiesis by increasing ACE NH2-terminal activity, Clin. Sci. 135 (2021) 2377–2391, https://doi.org/10.1042/CS20210739.

[46] J.S.R. Costa, G.F.A.C. Fonseca, N.C. dos S. Ottone, P.A. Silva, R.F. Antonaccio, G. Silva, M. da S.A. Rocha, C.C. Coimbra, E.A. Esteves, Z.A. Mang, F.T. Amorim, F. de C. Magalhães, Strength training improves insulin resistance and differently affects mitochondria in skeletal muscle and visceral adipose tissue in high-fat fed mice, Life Sci. 278 (2021), https://doi.org/10.1016/j.lfs.2021.119639.

[47] C.T. Liu, G.A. Brooks, Mild heat stress induces mitochondrial biogenesis in C2C12 myotubes, J. Appl. Physiol. 112 (2012) 354–361, https://doi.org/10.1152/japplphysiol.00989.2011.

[48] P.S. Hafen, C.N. Preece, J.R. Sorensen, C.R. Hancock, R.D. Hyldahl, Repeated exposure to heat stress induces mitochondrial adaptation in human skeletal muscle, J. Appl. Physiol. (2018), https://doi.org/10.1152/japplphysiol.00383.2018.

[49] H.W. Chen, S.C. Chen, J.L. Tsai, R.C. Yang, Previous hyperthermic treatment increases mitochondria oxidative enzyme activity and exercise capacity in rats, Kaohsiung J. Med. Sci. (1999), https://doi.org/10.6452/KJMS.199910.0572.

[50] A.A. Gupte, G.L. Bomhoff, R.H. Swerdlow, P.C. Geiger, Heat treatment improves glucose tolerance and prevents skeletal muscle insulin resistance in rats fed a high-fat diet, Diabetes 58 (2009) 567–578, https://doi.org/10.2337/db08-1070.

[51] J. Chung, A.-K. Nguyen, D.C. Henstridge, A.G. Holmes, M.H.S. Chan, J.L. Mesa, G. I. Lancaster, R.J. Southgate, C.R. Bruce, S.J. Duffy, I. Horvath, R. Mestril, M. J. Watt, P.L. Hooper, B.A. Kingwell, L. Vigh, A. Hevener, M.A. Febbraio, HSP72 protects against obesity-induced insulin resistance, Proc. Natl. Acad. Sci. USA 105 (2008) 1739–1744, https://doi.org/10.1073/pnas.0705799105.

[52] B.R. Ely, Z.S. Clayton, C.E. McCurdy, J. Pfeiffer, K.W. Needham, L.N. Comrada, C. T. Minson, Heat therapy improves glucose tolerance and adipose tissue insulin signaling in polycystic ovary syndrome, Am. J. Physiol. Endocrinol. Metabol. 317 (2019) E172–E182, https://doi.org/10.1152/ajpendo.00549.2018.

[53] A. Krook, R.A. Roth, X.J. Jiang, J.R. Zierath, H. Wallberg-Henriksson, Insulin-stimulated Akt kinase activity is reduced in skeletal muscle from NIDDM subjects, Diabetes (1998), https://doi.org/10.2337/diab.47.8.1281.

[54] J.R. Zierath, A. Krook, H. Wallberg-Henriksson, Insulin action in skeletal muscle from patients with NIDDM, Mol. Cell. Biochem. 182 (1998) 153–160, https://doi.org/10.1023/A:1006861628496.

[55] J.T. Brozinick, B.R. Roberts, G.L. Dohm, Defective signaling through Akt-2 and -3 but not Akt-1 in insulin-resistant human skeletal muscle: potential role in insulin resistance, Diabetes (2003), https://doi.org/10.2337/diabetes.52.4.935.

[56] H.K.R. Karlsson, J.R. Zierath, S. Kane, A. Krook, G.E. Lienhard, H. Wallberg-Henriksson, Insulin-stimulated phosphorylation of the Akt substrate AS160 is impaired in skeletal muscle of type 2 diabetic subjects, Diabetes 54 (2005) 1692–1697, https://doi.org/10.2337/diabetes.54.6.1692.

[57] D. Cozzone, S. Fröjdö, E. Disse, C. Debard, M. Laville, L. Pirola, H. Vidal, Isoform-specific defects of insulin stimulation of Akt/protein kinase B (PKB) in skeletal muscle cells from type 2 diabetic patients, Diabetologia 51 (2008) 512–521, https://doi.org/10.1007/s00125-007-0913-8.

[58] K. Højlund, J.B. Birk, D.K. Klein, K. Levin, A.J. Rose, B.F. Hansen, J.N. Nielsen, H. Beck-Nielsen, J.F.P. Wojtaszewski, Dysregulation of glycogen synthase COOH-and NH2-terminal phosphorylation by insulin in obesity and type 2 diabetes mellitus, J. Clin. Endocrinol. Metab. (2009), https://doi.org/10.1210/jc.2009-0897.

[59] K.T. Tonks, Y. Ng, S. Miller, A.C.F. Coster, D. Samocha-Bonet, T.J. Iseli, A. Xu, E. Patrick, J.Y.H. Yang, J.R. Junnutula, Z. Modrusan, G. Kolumam, J. Stöckli, D. J. Chisholm, D.E. James, J.R. Greenfield, Impaired Akt phosphorylation in insulin-resistant human muscle is accompanied by selective and heterogeneous downstream defects, Diabetologia (2013), https://doi.org/10.1007/s00125-012-2811-y.

[60] J. Shao, H. Yamashita, L. Qiao, J.E. Friedman, Decreased Akt kinase activity and insulin resistance C57BL/KsJ-Lepr(db/db) mice, J. Endocrinol. 167 (2000) 107–115, https://doi.org/10.1677/joe.0.1670107.

[61] F. Tremblay, C. Lavigne, H. Jacques, A. Marette, Defective insulin-induced GLUT4 translocation in skeletal muscle of high fat-fed rats is associated with alterations in

[62] both akt/protein kinase B and atypical protein kinase C (ζ/λ) activities, Diabetes (2001), https://doi.org/10.2337/diabetes.50.8.1901.

[62] H. Cho, J. Mu, J.K. Kim, J.L. Thorvaldsen, Q. Chu, E.B. Crenshaw, K.H. Kaestner, M.S. Bartolomei, G.I. Shulman, M.J. Birnbaum, Insulin resistance and a diabetes mellitus-like syndrome in mice lacking the protein kinase Akt2 (PKBβ), Science (1979), https://doi.org/10.1126/science.292.5522.1728, 2001.

[63] X.T. Feng, T.Z. Wang, J. Leng, Y. Chen, J.B. Liu, Y. Liu, W.J. Wang, Palmitate contributes to insulin resistance through downregulation of the src-mediated phosphorylation of Akt in C2C12 myotubes, Biosci. Biotechnol. Biochem. (2012), https://doi.org/10.1271/bbb.120107.

[64] J. Shao, H. Yamashita, L. Qiao, J. Friedman, Decreased Akt kinase activity and insulin resistance in C57BL/KsJ-Leprdb/db mice, J. Endocrinol. 167 (2000) 107–115, https://doi.org/10.1677/joe.0.1670107.

[65] N. Sharma, E.B. Arias, A.D. Bhat, D.A. Sequea, S. Ho, K.K. Croff, M.P. Sajan, R. V. Farese, G.D. Cartee, Mechanisms for increased insulin-stimulated Akt phosphorylation and glucose uptake in fast- and slow-twitch skeletal muscles of calorie-restricted rats, Am. J. Physiol. Endocrinol. Metabol. 300 (2011) E966–E978, https://doi.org/10.1152/ajpendo.00659.2010.

[66] J.J. Senn, Toll-like receptor-2 is essential for the development of palmitate-induced insulin resistance in myotubes, J. Biol. Chem. 281 (2006) 26865–26875, https://doi.org/10.1074/jbc.M513304200.

[67] R. Vijayvargia, K. Mann, H.R. Weiss, H.J. Pownall, H. Ruan, JNK deficiency enhances fatty acid utilization and diverts glucose from oxidation to glycogen storage in cultured myotubes, Obesity 18 (2010) 1701–1709, https://doi.org/10.1038/oby.2009.501.

[68] G.K. Bandyopadhyay, J.G. Yu, J. Ofrecio, J.M. Olefsky, Increased p85/55/50 expression and decreased phosphotidylinositol 3-kinase activity in insulin-resistant human skeletal muscle, Diabetes 54 (2005) 2351–2359, https://doi.org/10.2337/diabetes.54.8.2351.

[69] S.-H. Chiang, M. Bazuine, C.N. Lumeng, L.M. Geletka, J. Mowers, N.M. White, J.-T. Ma, J. Zhou, N. Qi, D. Westcott, J.B. Delproposto, T.S. Blackwell, F.E. Yull, A. R. Saltiel, The protein kinase IKKε regulates energy balance in obese mice, Cell 138 (2009) 961–975, https://doi.org/10.1016/j.cell.2009.06.046.

[70] R.K. Barr, M.A. Bogoyevitch, The c-Jun N-terminal protein kinase family of mitogen-activated protein kinases (JNK MAPKs), Int. J. Biochem. Cell Biol. 33 (2001) 1047–1063, https://doi.org/10.1016/S1357-2725(01)00093-0.

[71] F. Salehpour, F. Farajdokht, P. Cassano, S. Sadigh-Eteghad, M. Erfani, M. R. Hamblin, M.M. Salimi, P. Karimi, S.H. Rasta, J. Mahmoudi, Near-infrared photobiomodulation combined with coenzyme Q10 for depression in a mouse model of restraint stress: reduction in oxidative stress, neuroinflammation, and apoptosis, Brain Res. Bull. 144 (2019) 213–222, https://doi.org/10.1016/j.brainresbull.2018.10.010.

[72] R.T. Masha, N.N. Houreld, H. Abrahamse, Low-intensity laser irradiation at 660 nm stimulates transcription of genes involved in the electron transport chain, Photomed Laser Surg 31 (2013) 47–53, https://doi.org/10.1089/pho.2012.3369.

[73] L.M.D. Nguyen, A.G. Malamo, K.A. Larkin-Kaiser, P.A. Borsa, P.J. Adhihetty, Effect of near-infrared light exposure on mitochondrial signaling in C2C12 muscle cells, Mitochondrion 14 (2014) 42–48, https://doi.org/10.1016/j.mito.2013.11.001.

[74] R. Liu, P. Jin, L. Yu, Y. Wang, L. Han, T. Shi, X. Li, Impaired mitochondrial dynamics and bioenergetics in diabetic skeletal muscle, PLoS One (2014), https://doi.org/10.1371/journal.pone.0092810.

[75] B. Littlejohns, P. Pasdois, S. Duggan, A.R. Bond, K. Heesom, C.L. Jackson, G. D. Angelini, A.P. Halestrap, M.S. Suleiman, Hearts from mice fed a non-obesogenic high-fat diet exhibit changes in their oxidative state, calcium and mitochondria in parallel with increased susceptibility to reperfusion injury, PLoS One 9 (2014), https://doi.org/10.1371/journal.pone.0100579.

[76] D. Bach, D. Naon, S. Pich, F.X. Soriano, N. Vega, J. Rieusset, M. Laville, C. Guillet, Y. Boirie, H. Wallberg-Henriksson, M. Manco, M. Calvani, M. Castagneto, M. Palacin, G. Mingrone, J.R. Zierath, H. Vidal, A. Zorzano, Expression of Mfn2, the charcot-marie-tooth neuropathy type 2A gene, in human skeletal muscle: effects of type 2 diabetes, obesity, weight loss, and the regulatory role of tumor necrosis factor and interleukin-6, Diabetes 54 (2005) 2685–2693, https://doi.org/10.2337/diabetes.54.9.2685.

[77] T. Yu, J.L. Robotham, Y. Yoon, Increased production of reactive oxygen species in hyperglycemic conditions requires dynamic change of mitochondrial morphology, Proc. Natl. Acad. Sci. U.S.A. 103 (2006) 2653–2658, https://doi.org/10.1073/pnas.0511154103.

[78] V.L. Wyckelsma, I. Levinger, M.J. McKenna, L.E. Formosa, M.T. Ryan, A. C. Petersen, M.J. Anderson, R.M. Murphy, Preservation of skeletal muscle mitochondrial content in older adults: relationship between mitochondria, fibre type and high-intensity exercise training, J. Physiol. 595 (2017) 3345–3359, https://doi.org/10.1113/JP273950.

[79] P.A.S. White, L.M. Cercato, J.M.D. Araújo, L.A. Souza, A.F. Soares, A.P.O. Barbosa, J.M. de R. Neto, A.C. Marçal, U.F. Machado, E.A. Camargo, M.R.V. Santos, L. C. Brito, Modelo de obesidade induzida por dieta hiperlipídica e associada à resistência à ação da insulina e intolerância à glicose, Arq. Bras. Endocrinol. Metabol. 57 (2013) 339–345, https://doi.org/10.1590/S0004-27302013000500002.

[80] K.R. Short, M.L. Bigelow, J. Kahl, R. Singh, J. Coenen-Schimke, S. Raghavakaimal, K.S. Nair, Decline in skeletal muscle mitochondrial function with aging in humans, Proc. Natl. Acad. Sci. U.S.A. 102 (2005) 5618–5623, https://doi.org/10.1073/pnas.0501559102.

[81] H. Wang, J. Deng, W. Tu, L. Zhang, H. Chen, X. Wu, Y. Li, H. Sha, The hematologic effects of low intensity 650 nm laser irradiation on hypercholesterolemia rabbits, Am J Transl Res 8 (2016) 2293–2300.

[82] S. Larsen, J. Nielsen, C.N. Hansen, L.B. Nielsen, F. Wibrand, N. Stride, H. D. Schroder, R. Boushel, J.W. Helge, F. Dela, M. Hey-Mogensen, Biomarkers of mitochondrial content in skeletal muscle of healthy young human subjects, J. Physiol. 590 (2012) 3349–3360, https://doi.org/10.1113/jphysiol.2012.230185.

[83] R.A. Jacobs, V. Díaz, A.K. Meinild, M. Gassmann, C. Lundby, The C57Bl/6 mouse serves as a suitable model of human skeletal muscle mitochondrial function, Exp. Physiol. (2013), https://doi.org/10.1113/expphysiol.2012.070037.

[84] N. Ørtenblad, M. Mogensen, I. Petersen, K. Højlund, K. Levin, K. Sahlin, H. Beck-Nielsen, M. Gaster, Reduced insulin-mediated citrate synthase activity in cultured skeletal muscle cells from patients with type 2 diabetes: evidence for an intrinsic oxidative enzyme defect, Biochim. Biophys. Acta (BBA) - Mol. Basis Dis. 1741 (2005) 206–214, https://doi.org/10.1016/j.bbadis.2005.04.001.

[85] A.E. Aquino, M. Sene-Fiorese, C.A. Castro, F.O. Duarte, J.C. Oishi, G.C. Santos, K. A. Silva, F. Fabrizzi, G. Moraes, S.M.M. Matheus, A.C.G.O. Duarte, V.S. Bagnato, N. A. Parizotto, Can low-level laser therapy when associated to exercise decrease adipocyte area? J. Photochem. Photobiol., B 149 (2015) 21–26, https://doi.org/10.1016/j.jphotobiol.2015.04.033.

[86] W.H. de Brito Vieira, C. Ferraresi, M.L.B. Schwantes, S.E. de Andrade Perez, V. Baldissera, M.S. Cerqueira, N.A. Parizotto, Photobiomodulation increases mitochondrial citrate synthase activity in rats submitted to aerobic training, Lasers Med Sci 33 (2018) 803–810, https://doi.org/10.1007/s10103-017-2424-2.

[87] S. Guo, L. Gong, Q. Shen, D. Xing, Photobiomodulation reduces hepatic lipogenesis and enhances insulin sensitivity through activation of CaMKKβ/AMPK signaling pathway, J. Photochem. Photobiol., B 213 (2020) 112075, https://doi.org/10.1016/j.jphotobiol.2020.112075.

[88] M. Bonifacio, I.D. Benfato, M. de Almeida Cruz, D.C. de Sales, I.L. Pandolfo, H. T. Quintana, C.P. de F. Carvalho, C.A.M. de Oliveira, A.C.M. Renno, Effects of photobiomodulation on glucose homeostasis and morphometric parameters in pancreatic islets of diabetic mice, Lasers Med Sci (2021), https://doi.org/10.1007/s10103-021-03434-7.

[89] C.M.C.B. Scontri, F. de Castro Magalhães, A.P.M. Damiani, M.R. Hamblin, A. R. Zamunér, C. Ferraresi, Dose and time–response effect of photobiomodulation therapy on glycemic control in type 2 diabetic patients combined or not with hypoglycemic medicine: a randomized, crossover, double-blind, sham-controlled trial, J. Biophot. (2023), https://doi.org/10.1002/jbio.202300083.

[90] S.N. Linares, T. Beltrame, G.A.M. Galdino, M.C.M. Frade, J.C. Milan-Mattos, M. O. Gois, A. Borghi-Silva, P.F. de Biase, F.B. Manchado-Gobatto, V.S. Bagnato, N. A. Parizotto, C. Ferraresi, A.M. Catai, Dose response effect of photobiomodulation on hemodynamic responses and glucose levels in men with type 2 diabetes: a randomized, crossover, double-blind, sham-controlled trial, Photonics 9 (2022) 481, https://doi.org/10.3390/photonics9070481.

[91] M.B. Powner, G. Jeffery, Light stimulation of mitochondria reduces blood glucose levels, J. Biophot. 17 (2024), https://doi.org/10.1002/jbio.202300521.